Synthesis and Characterization of Magnetite Nanocomposites for Photocatalytic Reactions

A

Thesis Submitted

In partial fulfillment for the award of the degree for

MASTER OF SCIENCE

IN

CHEMISTRY

Submitted By:

Miss. Kamaljeet Kaur

(Reg. No. 301502015)

Under the supervision of:

Dr. Ashish Kumar

Lecturer

School of Chemistry and Biochemistry

Thapar University

July, 2017

CERTIFICATE

This is to certify that the project entitled ***"Synthesis and Characterization of Magnetite Nanocomposites for Photocatalytic Reactions"*** being submitted by Miss Kamaljeet Kaur in the partial fulfilment of requirement for the award of the degree of Masters of Science in the School of Chemistry and Biochemistry, Thapar University, Patiala, is an original work carried under the supervision of **Dr. Ashish Kumar**, Lecturer, School of Chemistry and Biochemistry, Thapar University, Patiala and no part of this project has been submitted for award of any other degree by me.

Kamaljeet Kaur

(Kamaljeet Kaur)

This is to certify the above statement made by student concerned is correct and true to the best of my knowledge.

Ashish Kumar

(Dr. Ashish Kumar)
Lecturer (Supervisor),
School of Chemistry and Biochemistry,
Thapar University, Patiala

CANDIDATE'S DECLARATION

I hereby declare that the work being presented in the dissertation entitled. ***"Synthesis and Characterization of Magnetite Nanocomposites for Photocatalytic Reactions"*** in partial fulfilment of the requirements for the award of the degree of Masters of Science in Chemistry, submitted in the School of Chemistry and Biochemistry, Thapar University, Patiala, is my own work during the period of January to July 2017, under the supervision of **Dr. Ashish Kumar,** Lecturer, School of Chemistry and Biochemistry, Thapar University, Patiala. My thesis has not previously formed the basis for award of any degree, or other similar title or recognition.

Date:

Place: Patiala

Kamaljeet Kaur.

(Kamaljeet Kaur)

This is to certify the above statement made by student concerned is correct and true to the best of my knowledge.

Ashish Kumar

(Dr. Ashish Kumar)
Lecturer (Supervisor),
School of Chemistry and Biochemistry,
Thapar University, Patiala

ACKNOWLEDGEMENTS

This dissertation would not have been possible without the guidance and help of several individuals who in one way or another contributed and extended their valuable assistance in the preparation and completion of this study.

First, and foremost, my gratitude to **Dr. Ashish Kumar**, Lecturer, School of Chemistry and Biochemistry, Thapar University, Patiala for his advice, supervision and crucial contribution which made him a backbone of this project work and so to this dissertation. The blessing, help and guidance given by him time to time shall carry me a long way in the journey of life on which I am about to embark.

A special word of appreciation for helpful and encouraging attitude of **Dr. Amjad Ali**, Associate Professor and Head, School of Chemistry and Biochemistry, Thapar University, Patiala for providing the necessary facilities.

My great sense of gratitude to **Mr. Rayees Ahmad Rather** for her support and guidance throughout the research work. I am highly thankful to all my lab mates especially, **Mr. Amit Mishra, Miss. Manisha Sharma, Miss. Akansha Mehta** and **Miss. Manpreet kaur** for providing helpful and cheerful environment during my project work.

I deeply appreciate the love, wishes and cooperation provided by **Miss Pooja Sharma** and **Mr. Bimal Kumar** for the successful completion of this project. Words are not enough to express my feelings about my immense gratitude that I owe to my family (**Mr. Jasvir Singh** and **Mrs. Sarbdeep Kaur**) and my brother (**Mr. Ajitpal Singh**) for their blessings and moral support. I would like to express my heartiest thanks to my dear friend **Miss Amanpreet Kaur** for her support and wishes for the successful completion of this project. Last but not the least I am thankful to all the persons who helped me directly or indirectly during the tenure of my project work.

Above all, I am grateful to GOD, Almighty who sustain this amazing world and without whose grace and blessings anybody can ever succeed.

Dated:

Place: Patiala

Kamaljeet Kaur

(Kamaljeet Kaur)

TABLE OF CONTENTS

ABSTRACT

The heterogeneous catalysis for photodegradation of cationic and anionic dyes was carried out by mesoporous magnetite nanoparticles (m-Fe_3O_4) and series of M containing magnetite nanoparticles where (M = CeO_2, TiO_2, SiO_2 and Au nanoparticles). m-Fe_3O_4 nanoparticles were synthesized by modified co-precipitation method with BET surface area 60.2 m^2g^{-1}. The M substituted nanocomposites were synthesized by hydrothermal method. The octahedral occupancy of M increased the BET surface area. Highest surface area was achieved with SiO_2/Fe_3O_4 was (120.5 m^2g^{-1}). Samples were characterized by XRD, FTIR, SEM, VSM and BET surface area. Methyl orange and methylene blue were chosen as model anionic and cationic dyes respectively for photodegradation studies. Photodegradation of methyl orange (90.4%) with CeO_2/Fe_3O_4 and methylene blue (91.4%) with SiO_2/Fe_3O_4 was achieved and it found to be efficient by using M/Fe_3O_4 NPs compared to the Fe_3O_4 alone. The M incorporation has significantly improves the catalytic activity of the magnetite nanoparticles. These new experiences are of high significance for the natural use of M substituted magnetite nanoparticles for the purification of industrial wastewater.

Introduction

1. INTRODUCTION

1.1 Nanotechnology and Nanoscience

Nanoscale science engineering and technology (NSET) is a new field that deals with the study and use of materials whose size falls into the nanometer range i.e. (less than 100 nm) [1]. The main important feature of Nanosciences and Nanotechnology is its "small size" which has opened up many opportunities for its development in all areas of science and engineering, including biotechnology, chemistry, material, energy, medicine, agriculture, food, electronic devices. Nanotechnologies are design to study an object at atomic, molecular and macromolecular level and also to study the applications, characterization and synthesis of structures by controlling their size and shape at nanometer scale (1-100) nm because in this range the conductivity, reactivity, electronic structure, freezing point, melting point, color, strength all these parameters can be measure with great potential. In 2000 the U.S, president Bill Clinton announced the creation of (NNI) i.e. National nanotechnology Initiative which had spent $22 billion for promoting many research and developing projects and set up the number of "Nanotech Companies" to make the people aware about this new field of science [2,3].

Table 1.1 Classification of nanomaterial on the basis of dimensions

Nanomaterial Dimensions	Examples
Three dimensions < 100nm	Quantum dots, nanorings, nanocapsules etc.
Two dimensions < 100nm	Nanotubes, fibers, nanowires etc.
One dimensions < 100nm	Thin films, layers, coating etc.

1.2 Magnetic Nanoparticles

In the recent years, the magnetic nanoparticles had gained great attention due to their electronic structure and optical properties. Iron oxide nanoparticles are highly pronounced magnetic nanoparticles. They exhibit numerous applications in water treatment, biomedicine, catalysis, cancer therapy and in many magnetic separation techniques [4,5]. Iron nanoparticles exist in three different form that are magnetite (Fe_3O_4), maghemite (γ-Fe_2O_3) and hematite (α-Fe_2O_3). Among all these oxides we have studied magnetite nanoparticles.

1.3 Magnetite (Fe_3O_4) Photocatalyst

1.3.1 Physical Properties of Magnetite (Fe_3O_4) Photocatalyst

Physical properties of magnetite: Density = 5.18 g/cm^3; Molecular Weight = 231.54 g; Melting Point = 1538 °C and Boiling Point = 2862 °C

Magnetite (Fe_3O_4) nanoparticles appear in the form of a dark brown powder with spherical morphology. Magnetite (Fe_3O_4) nanoparticles are ferromagnetic oxides having high surface area and also known as black iron oxide and loadstone. It is found in sedimentary rocks as fine grains with hardness of 5.5 to 6.5 in Mohs. It consists of both ferric (Fe^{3+}) and ferrous ($Fe^{2+)}$ species and exists as a monophasic material. It exhibit cubic inverse spinel structure with half of the Fe^{2+} ions occupy octahedral sites and remaining half of Fe^{3+} occupy tetrahedral sites [6]. Furthermore, due to electron delocalization effects magnetite can be slightly metal deficient on octahedral sites; such deficiency allows for n- and p-type magnetite semiconductors. Resultant conductivities range from 10^2–10^3 $\Omega^{-1}cm^{-1}$. Electrical conductivity evidence semiconductor behavior; however, this conductivity range borders conductor (metallic) behavior. Metals, semiconductors, and insulators historically exhibit bandgap ranging from 0.0, 0.2–3.0, >3.0 eV. Semi-metallic behavior is further supported by magnetite's relatively low bandgap (0.1 eV).

1.3.2 Effect of Metal Loading over Magnetite Nanoparticles

Great effort have made on surface modification of nanoparticles from last few decades just to improve their physical and chemicals properties [7]. Magnetite nanoparticles are highly prone to air as the particles get oxide on exposing to air and in aqueous solution get aggregated easier. So for its application in various potential fields surface modification is desirable for its stabilization [8]. From the past reports, it may concluded that doping of Fe_3O_4 with various non-magnetic, mesoporous, semiconductors materials enhance its stability, surface area, surface charge and electron density as well as increases the bandgap of Fe_3O_4.

The bandgap can be measured by UV-Visible spectroscopy and it is calculated by the equation:

$$\alpha h\upsilon = A\,(h\upsilon - E_g)$$

Where α is absorption coefficient, A is constant, h is planks constant, υ is photon frequency and E_g is band gap.

Introduction of metal and metal oxides over magnetite nanoparticles as we have used (Au and TiO_2, CeO_2, SiO_2) and observed the enhanced photocatalytic activity of anionic and cationic

dyes degradation. The activity of catalyst depends upon type of species and occupancy of substituent, as substitution with suitable metal oxide increases the generation of hydroxyl free radicals, which enhances the absorption of organic pollutants over the surface. In our experiment due to different absorption behavior of loaded metal oxides, the degradation of methyl orange and methylene blue occurred differently as observed by kinetic studies.

1.4 Applications of Magnetite Nanoparticles

- Magnetite nanoparticles exhibit various applications with great potential.
- Development of cost-effective nanoparticles for pollution detection, environment remediation has gained considerable attention.
- They used as a brilliant high surface area nano-absorbents for the removal of heavy metal ions mainly (Ag, As, Cd, Cr, Cu, Hg, Pb and Zn) and bacterial pathogens from the contaminated water as they are of using external magnetic field [9, 10].
- Magnetite nanoparticles also used as catalyst in many Fenton reactions occur in the presence of peroxide. It carry out Fenton oxidation of phenol [11], degradation of 4-chlorophenol [12].
- It is also carries out the degradation of many anionic, cationic and neutral dyes photo-catalytically because their magnetic properties allow their fast, inexpensive and easy separation from the reaction mixture [13, 14].
- Magnetite nanoparticles show application in tumor treatment also like thermal hyperthermia for cancer treatment [15]. These nanoparticles form conjugation with drug and improving drug delivery system. Drug/magnetite nanoparticles help in distributing drug in body, transferring to special location containing tumor. The advantage to using these particles is, to decreases the side effect of therapy arises from other treatment.

1.5 Photocatalysis

A photocatalyst is define as a substrate that is capable of absorbing light for the production of number of electron hole pairs without itself being destroyed or consumed. Photocatalysis is one of the most nonhazardous, ecofriendly, and economically feasible technologies that have been employed for its applications in purification of polluted air and water, self-cleaning glasses, tiles etc.

The photocatalytic process depends upon the bandgap between the conduction and valance band, high surface area, suitable morphology, stability and reusability of a catalyst.

Many metal oxides (e.g. TiO_2, Fe_2O_3, Fe_3O_4, and ZnS) are used as a photocatalyst for the degradation of the organic pollutants to carbon dioxide and water by reacting with oxygen under UV radiations [16].

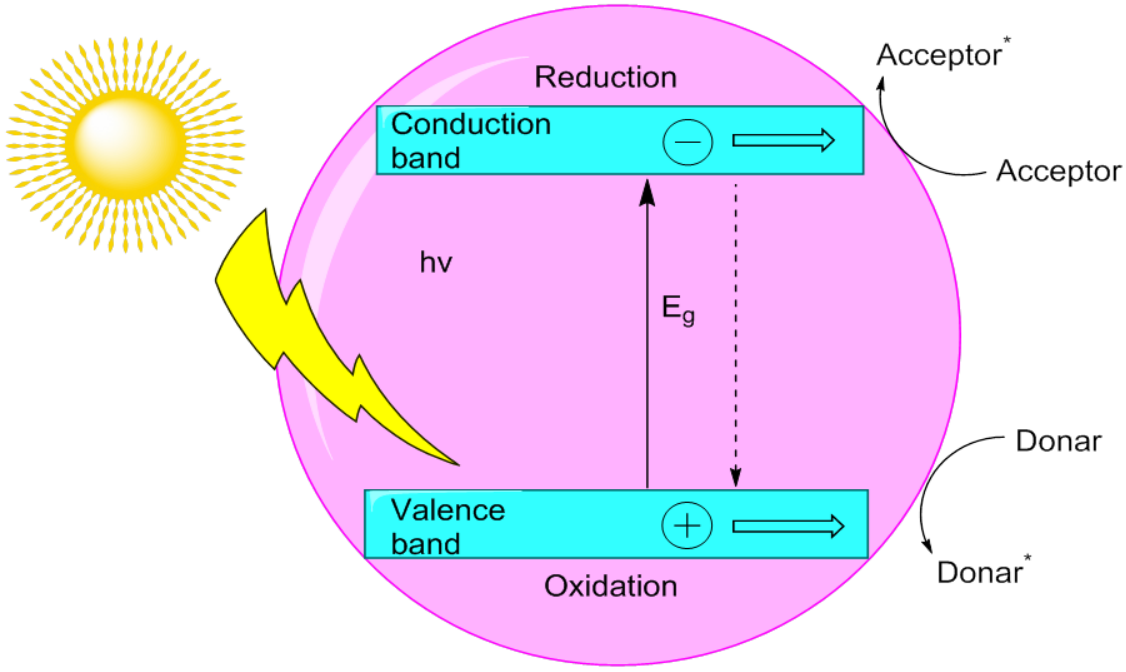

Figure 1. Mechanism of photocatalysis

The basic mechanism of photocatalysis involves the activation of metal oxides with UV/Visible radiations as a result of which an electron get promoted from the valence band to conduction band leaving behind a positive hole in the valence band. The energy of the incident photon required for the excitation of an electron depends upon the band gap of the specific material. Photo generated electron hole pairs migrate towards the catalyst surface and react with various absorbed pollutants.

$$\text{Photocatalyst} + h\nu \longrightarrow h^+ + e^-$$

In aqueous based suspension the holes in the valence band converts the water molecules and hydroxide ions into the hydroxyl radicals which are strong oxidizing species and capable of oxidizing organic contaminants into carbon dioxide and water.

$$H_2O + h^+ \longrightarrow \dot{O}H + H^+$$

The electrons in the conduction band react with the oxygen molecule leads to the formation of superoxide ion which is highly reactive species and capable of oxidizing organic pollutants.

$$O_2 + e^- \longrightarrow \dot{O}_2^-$$

1.6 Types of Photocatalysis

(1) **Homogeneous Photocatalysis:** The catalysis occurring in the presences of catalyst which is in the same phase from that, the reactants of the reaction mixture under suitable radiations. In homogeneous photocatalysis the catalysts have good selectivity for a single active site only; the recovery of the catalyst is very difficult and its thermal stability is also very poor.

(2) **Heterogeneous Photocatalysis:** The catalysis occurring in the presences of catalyst which is in the different phase from that, the reactants of the reaction mixture under suitable radiations. So it can be carried out in various media either in gas phase or in liquid phase. In heterogeneous photocatalysis the catalyst have good selectivity for multiple active sites, the recovery of the catalyst is very easy, and its thermal stability is high.

1.7 Importance of Heterogeneous Photocatalysis

In this experiment we use heterogeneous photocatalysis. In heterogeneous catalysis, one or more reactant molecules get absorbed at the active sites of the catalyst, hence interactions takes place between the surface of catalyst and the reactant molecules which makes it more reactive. At, this stage the reaction happens and product molecules get desorbed. It means the product molecules breaks away and leave the active site available for new set of molecules to get attach with it and react. It is a new advanced oxidation technology (AOT) for the treatment of industrial waste water with high degree of pollutants [17, 18]. Among several oxidation processes heterogeneous photocatalysis is one of the promising technology due to its outstanding ability in degrading wide range of organic pollutants in the waste water. In heterogeneous photocatalysis, the primary reaction involves the generation of the highly reactive hydroxyl radicals using semiconductor based photocatalyst like iron mixed oxide nanoparticles which are presently in this experiment under suitable light radiations.

Literature Review

2. Literature Review

An increased investigation was carried out in field of nano-sized magnetic particles in the last few years to synthesis various magnetic iron oxide nanoparticles such as hematite, magnetite and maghemite. Among all these magnetite has a unique properties and advantages due its low toxicity, low cost, good biocompatibility and strong magnetism so several methods has been proposed for its synthesis and to study its morphology. These methods involve co-precipitation [19-21], hydrothermal, sol-gel [22], self- assembly, and pulsed current electrochemical method.

Daou, T.J. et al. (2006)[23]

They have reported the synthesis of mono-disperse magnetite nanoparticles by hydrothermal method with average size of about 39 nm. Firstly particles were synthesized by co-precipitation method by using salts of ferrous and ferric ions at 70 °C then it is followed by hydrothermal method at 250 °C in teflon lined autoclave, because later prevent the oxidation of Fe^{2+} ions to Fe^{3+} ions that occurs in the co-precipitation method. In hydrothermal method the particles has high crystallinity and have ferromagnetic behavior at room temperature.

The nanoparticles were characterized carefully before and after applying hydrothermal treatment and the observed from X-ray data that before hydrothermal treatment the lattice parameter 'a' is intermediate between maghemite (γ-Fe_2O_3) and magnetite (Fe_3O_4) that means oxidation take place in the presence of air. Fe^{2+} ions because of their nano size get oxide to Fe^{3+} ions. After hydrothermal treatment the lattice parameter for crystalline phase is very close to magnetite.

Hassan, K. et al. (2013)[24]

Karami Hassan and his co-workers have proposed facial method for the synthesis of magnetite nanorods with average length and diameter of about 100 nm and 60 nm respectively by pulsed current electrochemical method using electrochemical cell containing three iron electrodes (one anode and two cathodes). Pulse of current is applied (18 mA cm^{-1}) to oxidize iron anode to iron oxide nanoparticles. They study the application of these nanorods as nonabsorbent in the purification of water by removing heavy metals such as Pd, Ni, Zn, Cu and Cd from it because water pollution by heavy metals occur globally [25]. They also check the reproducibility and stability of the magnetite nanorods by using them several times by same amount and also by monitoring the concentration of the iron.

Ranjbakhsh E. et al. (2012)[26]

In this study, the synthesis of silica coated Fe_3O_4 nanoparticles (17.5-21.0 nm) is reported for improving the stability and catalytic activity of lipase enzyme. Lipase is a water soluble enzyme; catalyze the hydrolysis of triacyl-glycerol to fatty acids and glycerol [27]. Firstly the synthesis of Fe_2O_3 was carried by co-precipitation method then silica SiO_2 coating was done by hydrothermal method. Their aim was to provide high surface area to lipase enzyme by incorporating porcine pancreas lipase (PPL) with NPs and enhance its catalytic activity.

Tian, Y. et al. (2011)[28]

Yang Tian and his co-workers has reported solvothermal method for mono-disperse Fe_3O_4 nano-crystals which is more convenient process then the popular thermal decomposition methods which requires inert atmosphere and reflux conditions. Iron acetylacetonate [$Fe(acac)_3$] is used as a precursor, reduced by *n*-octylamine in *n*-octanol as a solvent. The ratio of *n*-octylamine to *n*-octanol is varied to get 4 nm, 5 nm and 6 nm nanoparticles. As Fe_2O_3 nanoparticles have good biocompatibility, were then investigated by magnetic resonance imaging (MRI) with different particle size.

Li, H. et al. (2015)[29]

Haipeng Li and his co-workers design a synthesis to produce carbon-coated Fe_3O_4 nanoparticles forming core-shell composite with Fe_3O_4 particles 30 nm as cores and carbon 3-7 nm as shells. The synthesis was successfully carried out by hydrothermal method followed by the heat treatment as studied previously. These metal oxide composites due to their high discharge capacity 982 $mAhg^{-1}$ were used as a anode material in lithium-ion batteries to increase their specific capacities and energy densities.

Table 2.1 Fe_3O_4 nanoparticles synthesis, application and physical and chemical properties.

S. No.	Applications	Methods	Physical and Chemical Properties	References
1.	Monodisperse Fe_3O_4 for MRI imaging	Hydrothermal method	Average Size (AS) = 39 nm Saturation Magnetization (SM) = 82.5 emu/g	17
2.	Nanorods for removal of heavy metal ions	Pulsed current electrochemical method	Average Length (AL) = 900-1000 nm Diameter (D) = 60 nm SM = 89 emu/g	21
3.	SiO_2-Fe_3O_4 for improving catalytic activity of enzyme	Co-precipitation and hydrothermal method	AS = 17.5-21 nm SM = 53 emu/g	23
4.	Monodisperse Fe_3O_4 for MRI with different particle size	Solvothermal method	AS = 4 nm, 5 nm, 6 nm SM = 35.7-52.6 and 63.1 emu/g	26
5.	Core-shell composite of C-Fe_3O_4 for Li ion batteries	Hydrothermal method	AS = 30 nm (Fe_3O_4) Core thickness = 3-7 nm Discharge capacity = 982 mAh g^{-1}	27
6.	Nanochain assembly of magnetite(Fe_3O_4) for waste water treatment	One-pot surfactant free method	Chain length = 3-4 µm SA = 43.5 m^2g^{-1} SM = 82.1 emu/g	29
7.	Nano-flowers of Fe_3O_4 for bio medicinal application	Surfactant free hydrothermal method	AS = 30 nm SM = 66 emu/g	30
8.	Nano-composites of Fe_3O_4 with transition metal ions or organic pollutants	Hydrothermal method	Size = 10-40 nm SM = 32.6-57.5 emu/g	31
9.	Star shaped gold coated Fe_3O_4 for SERS detection	Co-precipitation followed by hydrothermal	AS = 33 -9 nm Diameter = 2.5 nm	32
10.	Cr-Fe_3O_4 as Fenton catalyst, for anionic/cationic dye degradation	Precipitation-oxidation method	Size = 15 nm SM = 37 emu/g	33

Min-Rui G. et al. (2011)[30]

Min-Rui Gao and his co-workers have reported the unique nanochains assemblies of magnetite (Fe_3O_4). The self-assembled chain is made of nano-flowers which are composed of nanoparticles. The particles with surface area (43.5 m^2g^{-1}), magnetization (82.1 emu/g) were obtained by one-pot surfactant free process using $Fe(acac)_3$ as a precursor. Due to excellent water dispersibility, nanochanins have wide applications in waste water treatment. The azo dye solution with initial concentration 100 mg/L is completely degraded by Fe_3O_4 at room temperature. These nanochains of Fe_3O_4 by simple heat treatment can be recycled and can be used for further application with same removal capability but low absorption rate.

Ramesh R. et al. (2012)[31]

They had designed the synthesis to produce nanoflowers of magnetite Fe_3O_4 of size 30 nm with super paramagnetic properties (66 emu/g). The synthesis was carried out through hydrothermal method by one pot process using TETA as a surfactant. Their aim was to study the effect of surfactant on the morphology of the particles and also to study the bio medicinal applications of the nanoflowers. Firstly the morphology of the particles was polyhedron, and then by varying the amount of TETA flower shaped particles were obtained.

Xiaoliang L. et al. (2013)[32]

Xiaoliang Liang and his co-workers studied the impact on the catalytic activity of the Fe_3O_4 nanoparticles by substituting its surface by some transition metal ion such as Ti^{4+}, V^{3+} andCr^{3+}. The application of doped Fe_3O_4 nanoparticles was then investigated in the degradation of organic pollutants (methylene Blue) photo-catalytically which requires the generation of hydroxyl free radicals. The doping of Fe_3O_4 particles with metal ions not only increase the surface area but it also enhance the generation of hydroxyl free radicals and thereby increase the absorption of MB on the surface of catalyst. The metal ions occupy the octahedral sites as they are highly exposed at the magnetite surface and take part in decomposition of H_2O_2 in generating free radicals. They worked on comparative study as they showed that among Ti^{4+}, $V^{3+}$and Cr^{3+}, titanium have great significant effect in improving the photocatalytic activity of magnetite nanoparticles.

In this present experiment, we had also worked on comparative study with our supporting material. The difference is doping of our support was done with metals and nonmetals.

Pedro Q. et al. (2014)[33]

Pedro Quaresma and his co-workers provided a novel method for the synthesis of gold coated magnetite star shaped nanoparticles (15 nm). The coating is done in two steps that involve the complete growth of the gold nuclei into star shaped shell. The obtained particles highly preserve the magnetic properties (37 emu/g) of the magnetite nanoparticles. The gold coating allows the bio-functionalization which is advantage for performing biological applications.

Xiaoliang L. et al. (2012)[34]

Xiaoliang Liang and his co-workers carried out the degradation of anionic and cationic dyes by Cr-Fe_3O_4 based heterogeneous Fenton catalyst under neutral pH conditions. The synthesis was carried out by simple precipitation-oxidation method. Methyl orange and methylene blue dye were chosen as pollutants. The effect of Cr doping was seen on the degradation efficiency of both the dyes by studying degradation kinetic.

In our present study also, we have seen the effect of substituent on magnetite Fe_3O_4 nanoparticles. The substitution was done with metals and non-metals for the degradation of methyl orange and methylene blue dye photo-catalytically.

Materials and Methodology

3. MATERIALS AND METHODOLOGY

The first part of the chapter deals with the basic theories and principles of materials and instruments that were used during the research work. This involves main analytical methods such as X-ray Diffraction (XRD), Fourier Transform Infrared Spectroscopy (FT-IR), BET surface area, Vibrating Sample Magnetometry (VSM), Dynamic Light Scattering (DLS), UV-Visible Spectrophotometer, Scanning Electron Microscopy-Energy Dispersive X-ray Spectrometry (SEM-EDS) which were used to study the morphology of the material. In the second part, the experimental procedures used for the synthesis of nanoparticles and its various nanocomposites are summarized.

3.1 MATERIALS

3.1.1 Reagents and Chemicals

All the chemicals used were purchased from Aldrich. In the present experiment, we have used ferrous (Fe^{2+}) and ferric (Fe^{3+}) salts of sulphonate ions as precursor. These salts are present in several hydrated forms and are highly soluble in water. Freshly prepared ammonium hydroxide (NH_4OH) was used as a precipitating agent.

3.1.2 Dyes

Methyl Orange

Methyl orange is an acidic dye with general molecular formula $C_{14}H_{14}N_3NaO_3S$. It belongs to the azodyes with brilliant orange colour which never fades fast to light. It is synthesized by coupling of dimethylaniline with diazotized sulphonilic acid. Its *p*ka value in water is 3.47 at 25 °C. In acidic solution, it is reddish, whereas in basic it exhibit yellow colour.

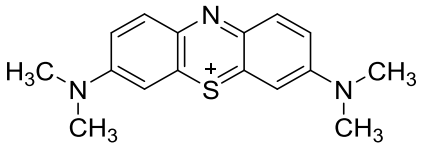

Figure 3.1: Structure of methyl orange dye

Methylene Blue

Methylene blue is a dark green crystal dye with bronze like luster. It is also known as methylthioninium chloride with molecular formula $C_{16}H_{18}ClN_3S$. It is basic in nature. The colour of methylene blue is deep blue in water and alcoholic solution.

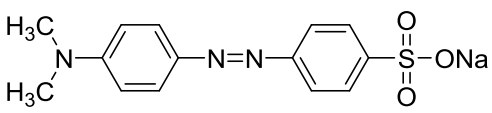

Figure 3.2: Structure of methylene blue dye.

3.2 APPARATUS

Beakers (50 mL and 250 mL), burette stand, test tubes (10 mL), round bottom flask (250 mL), pH paper or pH meter, test tube stand, micro pipette, measuring cylinder (10 mL and 100 mL), filter paper, magnetic beads, glass rod, plastic graduated centrifuge tubes (50 mL), petri dish, flasks (50 mL), pestle and mortar, crucible, dropper, spatula.

3.3 INSTRUMENT USED

3.3.1 Magnetic Stirrer

A magnetic stirrer of REMI 2MLH is used as a laboratory device. It consists of a hot plate; provide heating to the reaction mixture. The mixing process occurs only when a bar magnet is put into the reaction mixture because it works on the principle that, it uses magnetic field to rotate the magnetic bead and mix all the samples.

3.3.2 Weighing Balance

Weighing balance was used to measure the accurate weight of the chemicals used. Maximum 250 gm; Denisty-0.01 mg

3.3.3 Hot Air Oven

Hot air oven was used to dry the precipitates of obtained nanoparticles. Temperature can be controlled by using thermostat and operating it between 500 °C - 3000 °C.

3.3.4 Laboratory Centrifuge

The sedimentation of heterogeneous mixture by centrifugal force is known as centrifugation. Centrifugation is done to separate the two immiscible liquids. It works on the principle, where it allows radical motion of denser substances in the outward direction, displaced the less dense substances and make them move towards centre.

3.3.5 Muffle Furnace

A muffle furnace is used for it’s for its high temperature application. It is used by chemist in various research labs for non-volatile and non-combustible samples. It consist of highly heated chamber, which is used to carried out calcination of the sample at different temperatures without in contact with flame. It can be operated for maximum temperature of about 600 °C.

3.3.6 Autoclave

200 mL teflon lined autoclave is used as a laboratory reactor for caring out crystalline process by hydrothermal method. Where, solvent is treated under high pressure and temperature conditions. Teflon lining can bear high pressure and high temperature.

3.3.7 UV-Visible Spectrophotometer

UV-Visible spectrophotometer is used to study the absorption spectroscopy of the sample of our interest in the ultraviolet-visible region. It is used to determine different species such as highly conjugated organic compounds, transition metal ions and biological macromolecules. It is usually carried in liquid phase, uses light in the visible range which affects the colour of the substance involved. The principle on which it works is, molecules containing π electrons or non-bonding electrons can absorb light in the UV-visible range to excite electrons to the higher energy level. Lower the band gap, higher will be the wavelength of absorbed light.

$$A=\log 10\ (Io/I) = \in .c.l$$

It is based upon beer-Lambert law, according which absorbance of solution is related to the path length and the concentration of the absorbing species. Thus concentration can be determined through absorption calibration curve.

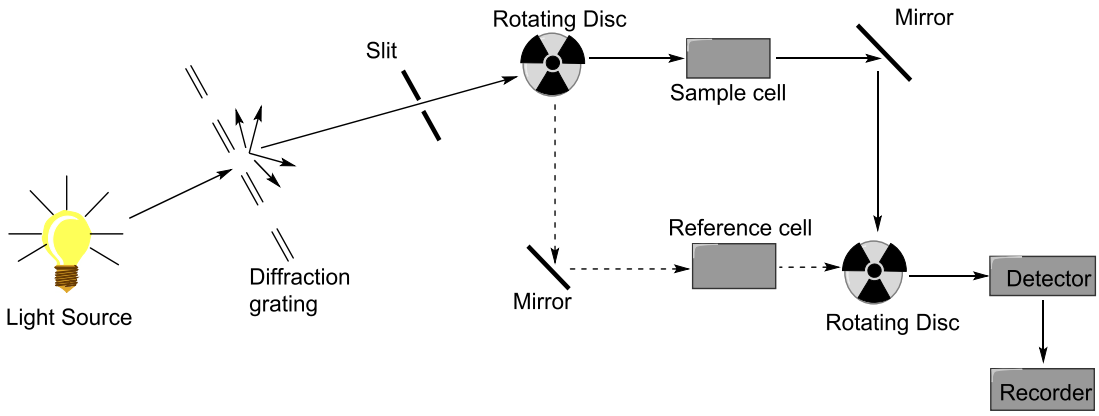

Figure 3.3: UV-Visible spectrophotometer

3.4 METHODOLOGY

3.4.1 Preparation of Fe_3O_4 Nanoparticles

Magnetic support was prepared by co-precipitation method by the following described method.

Step 1: In 500 mL beaker, equipped with hot plate and magnetic stirrer, 3.5 g of $FeSO_4.7H_2O$ and 10 g of $Fe_2(SO_4)_3$ were dissolved in 150 mL deionized water.

Step 2: To this solution, freshly prepared ammonia solution was added drop-wise at 65 °C with vigorous stirring, to maintain the final pH of 12.

Step 3: The mixture was stirred for 2 h, to obtain black precipitates of Fe_3O_4 nanoparticles.

Step 4: Washing was done with distilled water with the help of laboratory centrifuge, until the pH of supernatant becomes 7.

Step 5: Dry the precipitates in the microwave over for overnight at 60 °C.

Step 6: Finally the dye sample were calcined at 300-500 °C in the muffle furnace for 2-3 h.

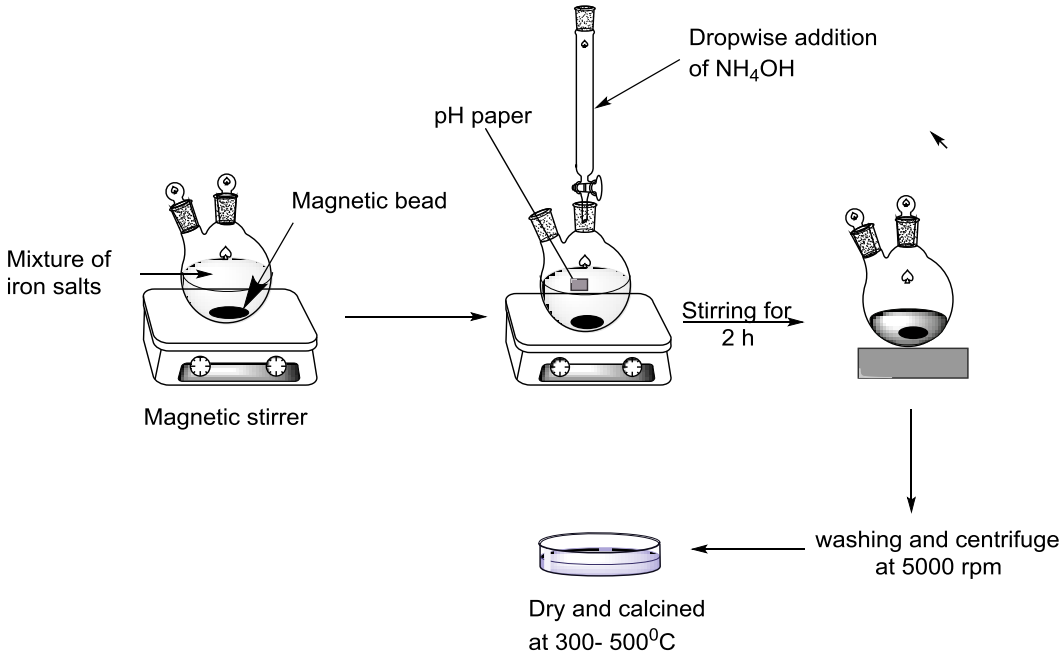

Figure 3.4: Synthesis of magnetite nanoparticles

3.4.2 Preparation of Metal and Metal Oxides

Titanium oxide (TiO_2): Titanium (IV) isopropoxide was used as a precursor for the synthesis of mesoporous TiO_2. Hydrolysis of titanium isopropoxide in the presence of 2-propanol and water at room temperature and continuous stirring for 1 h resulted in the formation of Titanium Hydroxide. The molar ratios of Ti/2-propanol/H_2O were 1:22:5 and volume (mL) ratios are 10:60:3. Ageing of precipitates was done at 80 ^oC. Precipitates were dried in oven at 100 ^oC. Finally, the dried samples were calcined at 400 ^oC for 4 h at a heating rate of 1 ^oC/ min.

Cerium oxide (CeO_2): $CeCl_3.7H_2O$ (2.0 mmol) was added slowly to the solution of L-glycine (4.1 mmol) and H_2O (10 mL) under continuous stirring. To the above solution was added 10 mL of 0.15 M $Na_2(CO_2)_2$ to obtain cerium oxalate as white precipitates. Finally, the

solution and the precipitates were transferred to an autoclave, which was sealed tightly and treated hydrothermally at 160^{o}C for 24 h in a hot air oven. The sample was collected through filtration; washing of precipitates was done with water and ethanol. The precipitates were dried at 60 ^{o}C for 12 h, calcined at 360^{o}C for 1 h, resulted in yellow coloured ceria powder.

Gold (Au) Nano-catalyst: The preparation of Au nano-catalyst was done by homogeneous deposition precipitation (HDP) method. In this method, the mixture of urea and aqueous solution of $HAuCl_4.3H_2O$ was stirred and heated up to 95 ^{o}C for 6 h. The urea decomposes to ammonia on heating resulting in the precipitation in a homogeneous way as the pH shift towards the basic range (pH 6-8). The precipitates were dried at 100 ^{o}C for 5 h.

Silicon dioxide (SiO_2): Silica (SiO_2) was commercial available (AKZO, Netherlands, grade Si 4-5P) were used for the synthesis of SiO_2/Fe_3O_4.

3.4.3 Synthesis of Magnetite Nanocomposites

Magnetite nanocomposites were synthesized by hydrothermal method. The process involves 1 g of Fe_3O_4 and 1 g of nano materials prepared above for coating was mixed in 40 mL of ethanol. The suspension was dispersed under ultrasonication for 20 min to obtain homogeneous mixture. After ultrasonication the mixture was then poured into teflon lined stainless autoclave. The autoclave was the put into a muffle furnace for 7-8 h at 350 °C. Then slowly cool the autoclave at room temperature naturally. The precipitates are then dried in oven and calcined at 450 °C for 2-3 h again in muffle furnace.

3.5 PHOTOCATALYTIC REACTIONS

3.5.1 Monitoring UV-Visible spectra of Degradation of methyl orange and methylene blue using mesoporous Fe_3O_4 as photocatalyst

Procedure

1. In a volumetric flask, Stock solution was prepared by dissolving 20 mg of dye in 1 L of deionized water in volumetric flask.

2. In a beaker 10 mL of above solution was taken and 10 mg of each catalyst was used.

Reaction in dark

3. Beaker was placed in dark on stirrer. At regular intervals of 2 min sample was withdrawn from the beaker for taking readings using UV spectrophotometer.

4. To remove catalyst from the liquid phase, filtration through 0.22 μm nylon syringe filters was done.

Reaction in visible light

5. The degradation of both the dyes was checked in the presence of sunlight for that beaker containing the dye solution and catalyst after reaction in dark was placed under solar energy. At regular intervals of 5 min sample was withdrawn from the beaker for taking reading using UV spectrophotometer.

6. To remove catalyst from the liquid phase, filtration through 0.22 μm nylon syringe filters was done.

Characterization Techniques

4. CHARACTERIZATION TECHNIQUES

4.1 X-Ray Diffractometer (XRD)

The sample was characterized in the range of 2θ = 10˚-80˚ by using XRD PAN ANALYTICAL X'PERT PRO diffractometer operating at 45KV and Cu Kα wavelength of 1.54 Å.

4.2 Fourier Transform Infrared Spectroscopy (FT-IR)

FT-IR was done to further confirm the formation of Fe_3O_4 and its different metal oxide nanocomposites. FT-IR of samples was carried out at 600 FT-IR spectrophotometer.

4.3 Scanning Electron Microscopy - Energy Dispersive X-ray Spectrometry (SEM-EDS)

A SEM is used to produce images of sample, by illuminating the sample with focused beam of electrons. It is type of electron microscopy, in which electrons interact with the atoms in a sample. These interactions result in the production of signals that gives information about samples surface composition and topography. Energy dispersive spectroscopy, JOEL JSM-7600F, 01operated at 30KV was carried at on SEM-EDS.

4.4 BET Surface Area

The theory of adsorption proposed by Brunauer, Teller and Emmett in 1938 is known as BET theory. The specific surface area of a mesoporous Fe_3O_4 and its various metal oxides had determined by physical adsorption of N_2 gas on surface of catalyst and by calculating the degree of adsorbate gas which absorbed as a monomolecular layer on the catalyst surface. Weak Vander Waals forces between the adsorbent surface and adsorbate gas molecules results in physical adsorption and also results in the formation of multilayers, which is true picture of adsorption.

Adsorption isotherms can be classified as one of 6 types, as shown in the Table 4.1.

BET equation:

$$q = \frac{q_m K_b C}{[C_a - C]\{1 + [K_b - 1][C / C_a]\}}$$

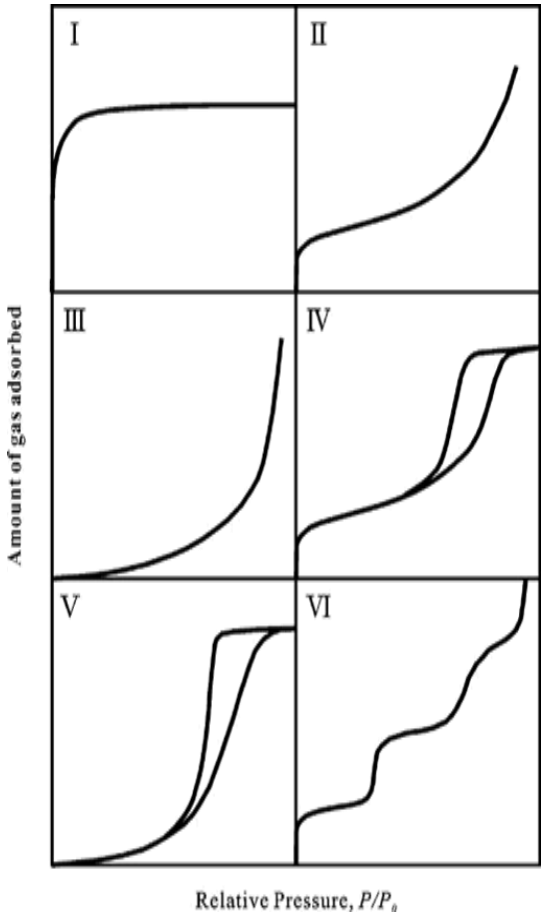

Figure 4.1: Types of adsorption isotherm

Table 4.1: Feature of adsorption isotherm

Type	Interaction between sample surface and adsorbate	Porosity	Sample- adsorptive example
I	Relatively strong	Micropores	Activated carbon-nitrogen
II	Relatively strong	Nonporous	Oxide-nitrogen
III	Weak	Nonporous	Carbon - water vapor
IV	Relatively strong	Mesopores	Silica-nitrogen
V	Weak	Mesopores	Activated carbon- water vapor
VI	Relatively strong	Nonporous	Graphite - krypton

Table 4.2: Sizes of pores classified as

Type	Pore diameter/nm
Micropore	< 2
Mesopore	2-50
Macropore	>50

4.5 Vibrating Sample Magnetometry (VSM)

To study the magnetic properties of the prepared samples, magnetic measurements were performed using VSM technique at 300K temperature. It is invented by Simon Foner in 1955 at MIT Lincoln Laboratory and reported in 1959. It uses external magnetic field and give us an M-H curve or hysteresis curve which depict the magnetization changes due to applied external magnetic field. Based upon the curve we get the desired data like coercivity (H_C), magnetic susceptibility (χ_i).

4.6 Differential Light Scattering (DLS)

It is a technique that commonly used in physics to determine the size distribution profile of small sized particles in solution or in suspension. It is based on the principle of Doppler shift and Brownian motion to determine the number of particle and hydrodynamic size in the suspension. The sample is illuminated by a laser beam, light gets scattered in all directions due to the Brownian motion of particles. These fluctuations of the scattered light are detected with the help of fast photon detector, which is able to detect the scattered light in its direction at known scattering angle Θ and give the average particle size in the limited size range.

Results & Discussion

5. RESULTS AND DISCUSSION

Based upon the composition of various samples of mesoporous M/Fe_3O_4 catalysts were characterized with the help of different techniques and the respective results were discussed as follows**.**

5.1 CATALYST CHARACTERIZATION

5.1.1 XRD Analysis

The XRD patterns of synthesized Fe_3O_4 nanoparticles and its nanocomposites with various metal oxides are shown in Figure 5.1. In case of pure magnetite particles four peaks occurs corresponding to standard Bragg reflection (220), (311), (400), (511) and (440) at 2Ɵ values (30.06, 35.42, 43.05, 57.15 and 62.79) respectively are shown in each figure. These diffraction peaks completely corresponds to face centered cubic lattice of crystalline Fe_3O_4 nanoparticles.

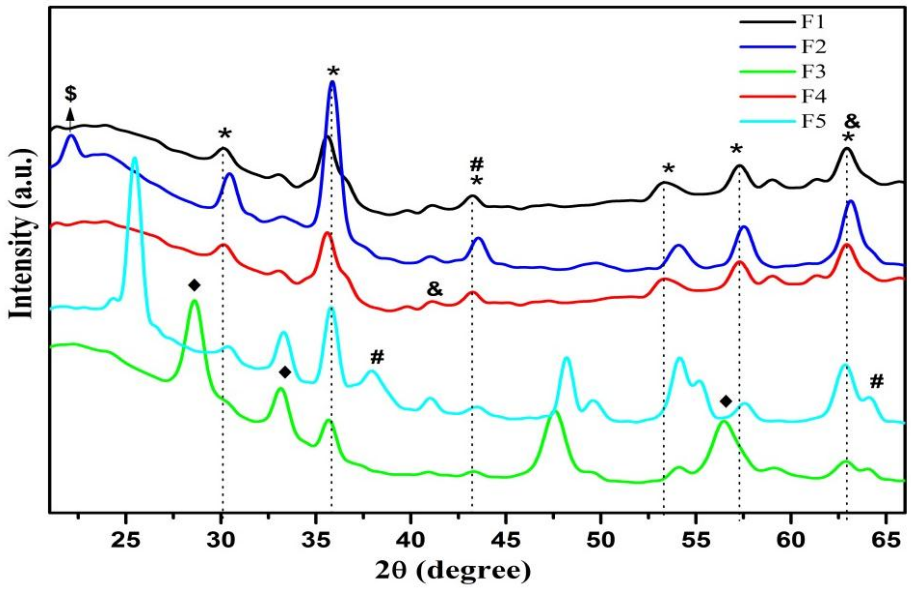

Figure 5.1: XRD patterns of Fe_3O_4 nanoparticles and its various nanocomposites.

F1 (Fe_3O_4), F2 (m-CeO_2/Fe_3O_4), F3 (SiO_2 /Fe_3O_4), F4 (m-TiO_2/Fe_3O_4) and F5 (Au/Fe_3O_4)
(*) (represents Fe_3O_4 peaks), **($)** (represents CeO_2 peaks), **(♦)** (represents SiO_2 peaks), **(#)** (represents M-TiO_2peaks) and **(&)** (represents Au peaks)

Symbols	compound	JCPDS No.
*	Fe_3O_4	19-0629
$	m-CeO_2	65-5923
♦	SiO_2	46-1045
#	m-TiO_2	76-1940
&	Au	01-1174

5.1.2 SEM-EDS and Mapping

The morphology of pure magnetite and its nanocomposites was characterised by SEM analysis. This gives the irregular morphology of pure mesoporous spherical shaped of Fe_3O_4 nanoparticles. The morphology of other nanocomposites is also spherically distorted as shown in Figure 5.3.

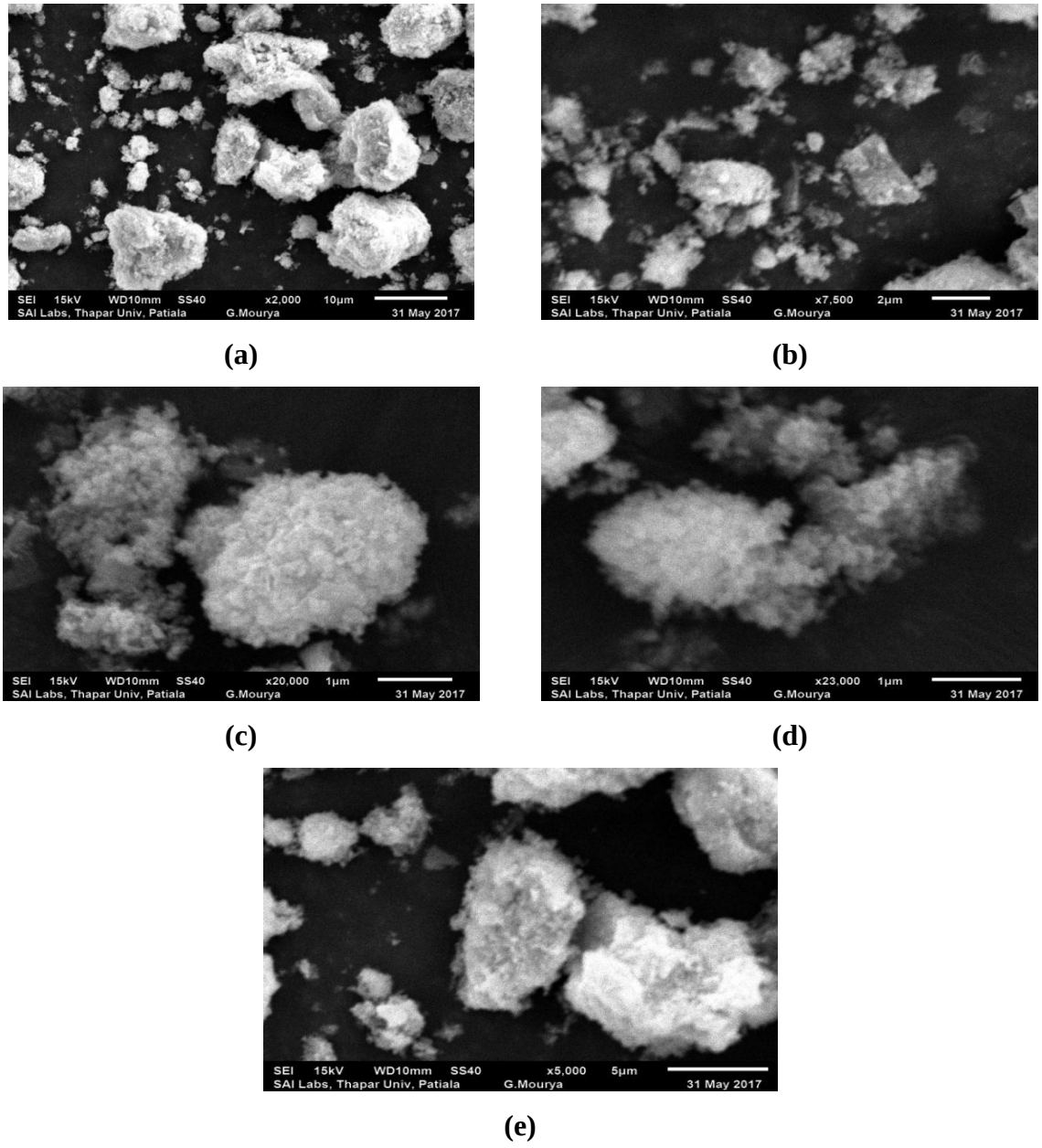

Figure 5.3: SEM images of (a) F1 (Fe_3O_4) and various supported catalysts (b) F2 (m-CeO_2/Fe_3O_4), (c) F3 (SiO_2 /Fe_3O_4), (d) F4 (m-TiO_2/Fe_3O_4), (e) F5 (Au/Fe_3O_4)

Energy dispersive analysis (EDS) gives the elementary information of the prepared sample. The spectra reveal the deposition of CeO_2 onto Fe_3O_4 in nearly equimolar ratio. This also confirms the existence of Fe_3O_4 and weight percentage of prepared catalyst.

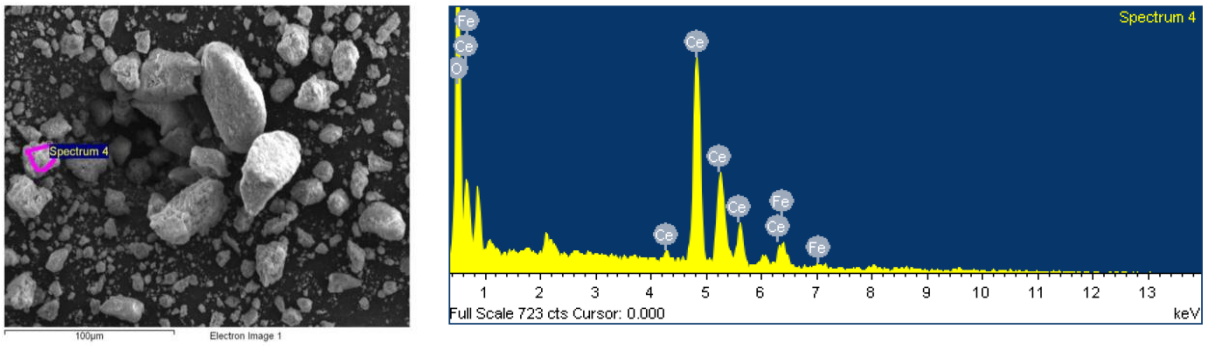

Figure 4: SEM EDEX analysis of m-CeO_2/Fe_3O_4 catalyst

Element	Weight %	Atomic %
O K	24.19	71.77
Fe K	4.98	4.23
Ce L	70.83	24.00

5.1.3 BET Surface area

In all cases, irregular spherical shaped samples with an interconnected mesoporous structures were obtained. The N_2 sorption isotherms of synthesized mesoporous Fe_3O_4 with different metal loading are shown in Figure 5.5. It is clearly shown that the relative pressure (P/Po) at which increase in the adsorption was observed, was shifting to higher values with different metal substituent. The BET surface area increased from 60 m^2g^{-1} to 120 m^2g^{-1}. The uniformity of pore sizes were defined by the sharp adsorption and desorption branches in hysteresis loops (a) and it varies from (16-20 nm). On the other hand, pore volume of the pure magnetite and its composites was significantly varied due to the variation of mesopores size (0.2 – 0.5 cm^3g^{-1}). BJH pore size distribution curve is also shown in Figure 5.5 (b)

Table 5.1: Nitrogen adsorption-desorption parameters showing effect of different metal oxides over the surface of Fe_3O_4

Sample Name	Surface Area (m^2g^{-1})	Pore Volume (cm^3g^{-1})	Pore Size (nm)
F1	60.2	0.2124	16.03
F2	120.5	0.5651	16.15
F3	99.5	0.3148	17.37
F4	71.6	0.6230	20.40
F5	78.6	0.4723	17.14

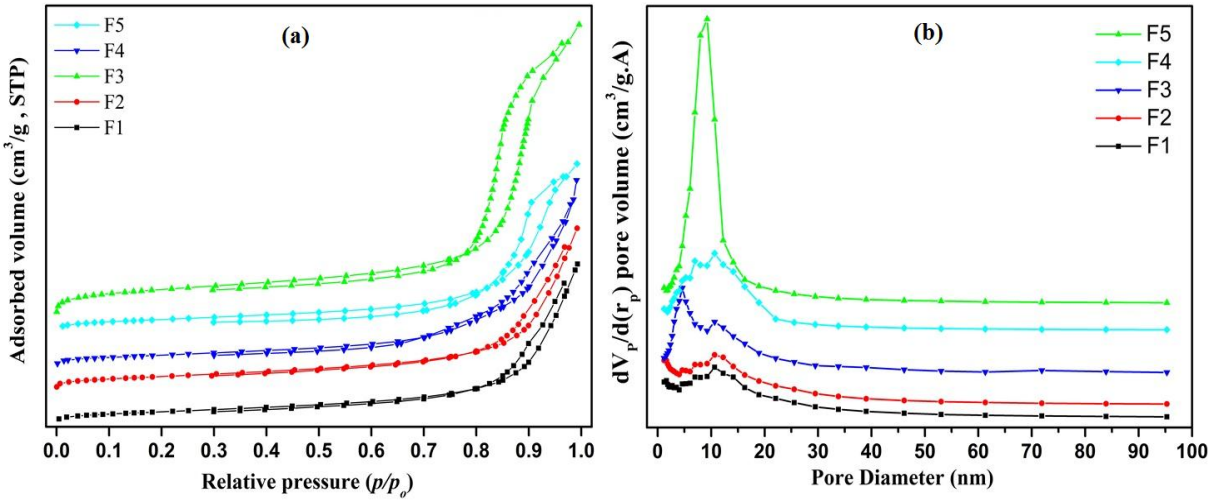

Figure 5.5: (a) N_2 adsorption-desorption isotherms; **(b)** BJH pore size distribution curves of F1 (Fe_3O_4) and various supported catalysts F2 (m-CeO_2/Fe_3O_4), F3 (SiO_2/Fe_3O_4), F4 (m-TiO_2/Fe_3O_4), F5 (Au/Fe_3O_4)

5.1.4 VSM Analysis

Magnetic analysis on pure sample as well as its nano-composites reveals that these particles having super paramagnetic structure with high magnetic saturation (M_s) with a maximum value of 36.59 emu/g in case of pure magnetite nanoparticles. The decrease in magnetization is also observed with different metal loading in Table 5.2 due to occupancy of octahedral and tetrahedral by different metal oxide which changes the interactions in pure Fe_3O_4 nanoparticles.

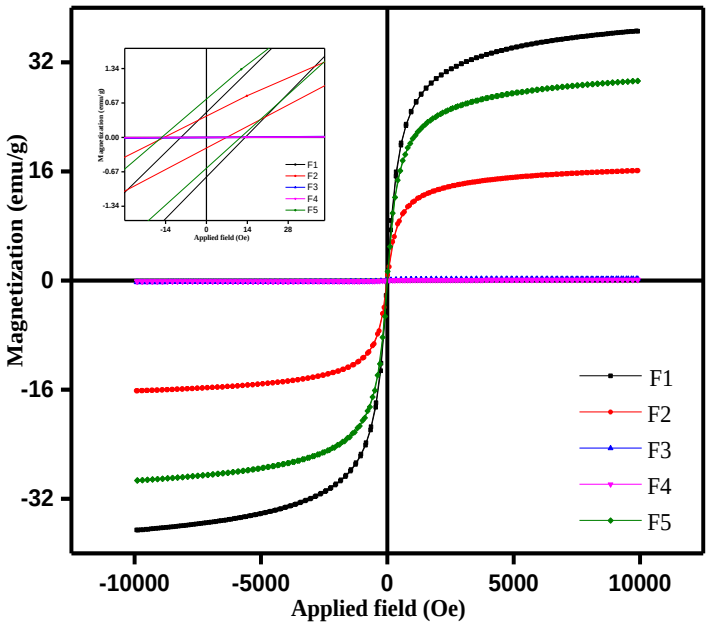

Figure 5.6: M-H curves of metal supported magnetite nanoparticles at room temperature.

Table 5.2 Magnetic parameters obtained from VSM analysis

Sample	M_s (emu/g)	M_r (emu/g)	H_c (Oe)
F1	36.59	1.11	11.17
F2	16.11	0.415	10.76
F3	0.225	0.019	15.03
F4	0.117	0.025	15.69
F5	29.26	0.746	13.68

5.1.5 DLS Analysis

DLS data showed that the average hydrodynamic size of Fe_3O_4 is nearly 100 nm as shown in Figure 5.7, whereas the size increases with metal loading. The zeta potential value for Fe_3O_4 is highly positive value, suggested that the magnetite nanoparticles has positive charge on the surface. The value of zeta potential becomes negative with metal loading and it is highly negative for F3. It means now the surface of the catalyst carry negative charge.

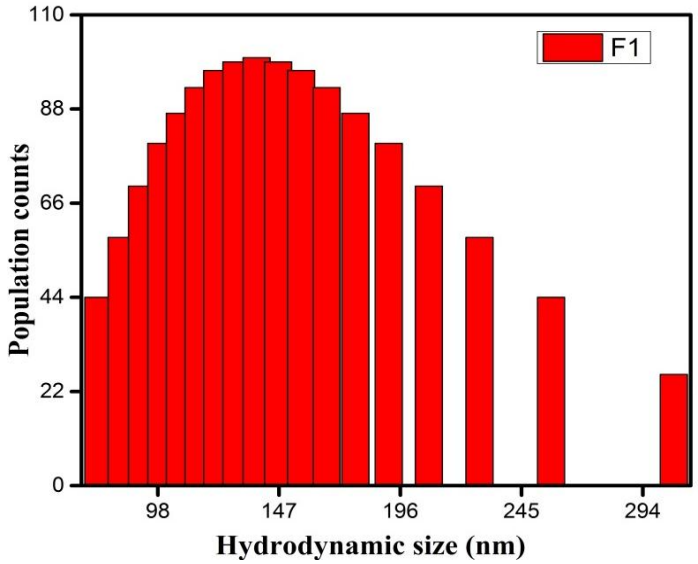

Figure 5.7: DLS spectrum of magnetite nanoparticles

Table 5.3: Zeta potential for the all sample.

Sample type	Zeta potential (mV)	Result quality
F1	12.5	Good
F2	-2.6	Good
F3	-19.1	Good
F4	-9.3	Good
F5	-8.58	Good

5.1.6 FTIR

FT-IR spectrum of pure Fe_3O_4 and M-Fe_3O_4 nanoparticles is demonstrated in Figure 5.8. In the pure sample , the presence of absorption bands at 544,794 and 900 cm^{-1} wavenumbers associated with Fe-O stretching vibrations of Fe^{2+} and Fe^{3+} ions in the octahedral sites and those of Fe^{3+} ions in the tetrahedral sites confirms the structure of Fe_3O_4 formation.

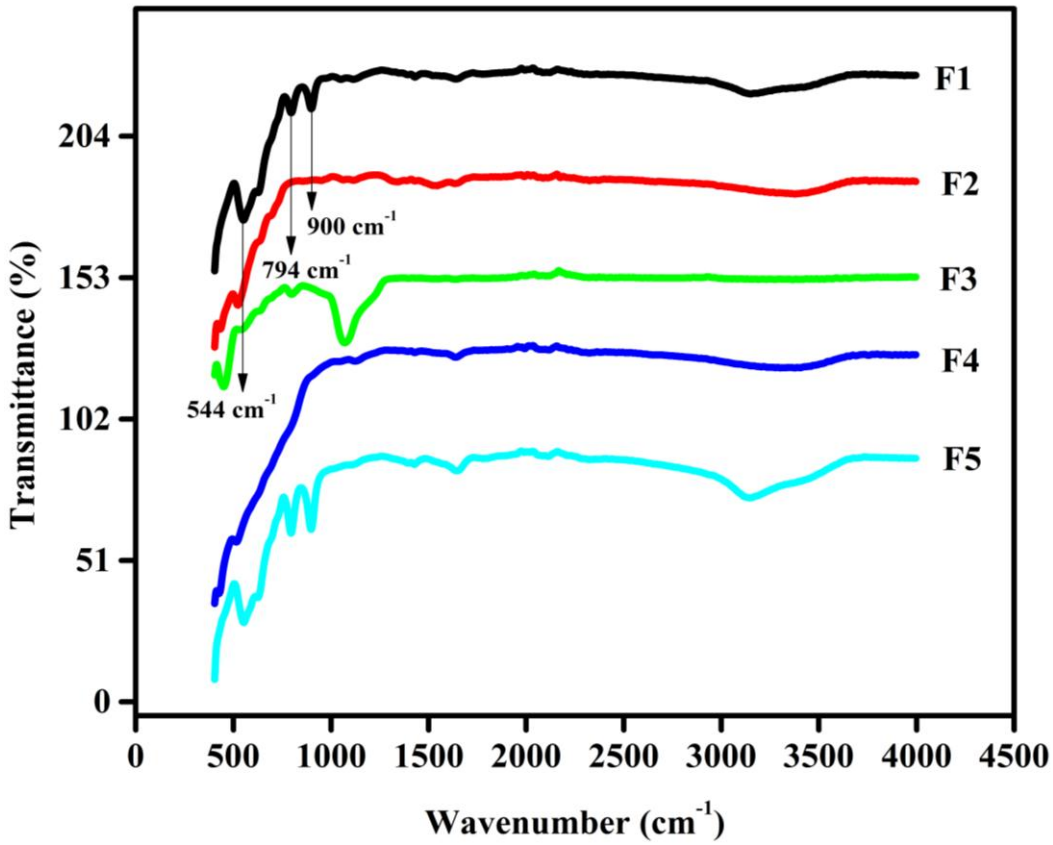

Figure 5.8: FTIR of (a) F1 (Fe_3O_4) and various supported catalysts (b) F2 (m-CeO_2/Fe_3O_4), (c) F3 (SiO_2 /Fe_3O_4), (d) F4 (m-TiO_2/Fe_3O_4), (e) F5 (Au/Fe_3O_4).

The shift happening at the wavelength range of 578-591 cm^{-1} with the substitution over the surface of Fe_3O_4 NPs. In all FTIR spectrums demonstrated in the Figure 5.8 two absorption band centered at 1624 and 3432 cm^{-1} can also be seen which corresponds to the O-H vibrations of the free water molecules and adsorbed water on samples' surface.

5.2 PHOTOCATALYTIC DEGRADATION STUDY

The photocatalytic activity and kinetics study in terms of Langmuir Hinshelwood model for degradation of methyl orange (anionic) and methylene blue (cationic) dyes is generally represented graphically. Each graph represents the catalytic efficiency of Fe_3O_4 and other supported metal oxides under visible light irradiations. Pure magnetite nanoparticles (Fe_3O_4) show low activity as compare to the mixed phase. However, the photocatalytic activity increases with gradual increase in metal content by loading in molar ratio1:1 over prepared Fe_3O_4.

Methyl Orange (cationic dye)

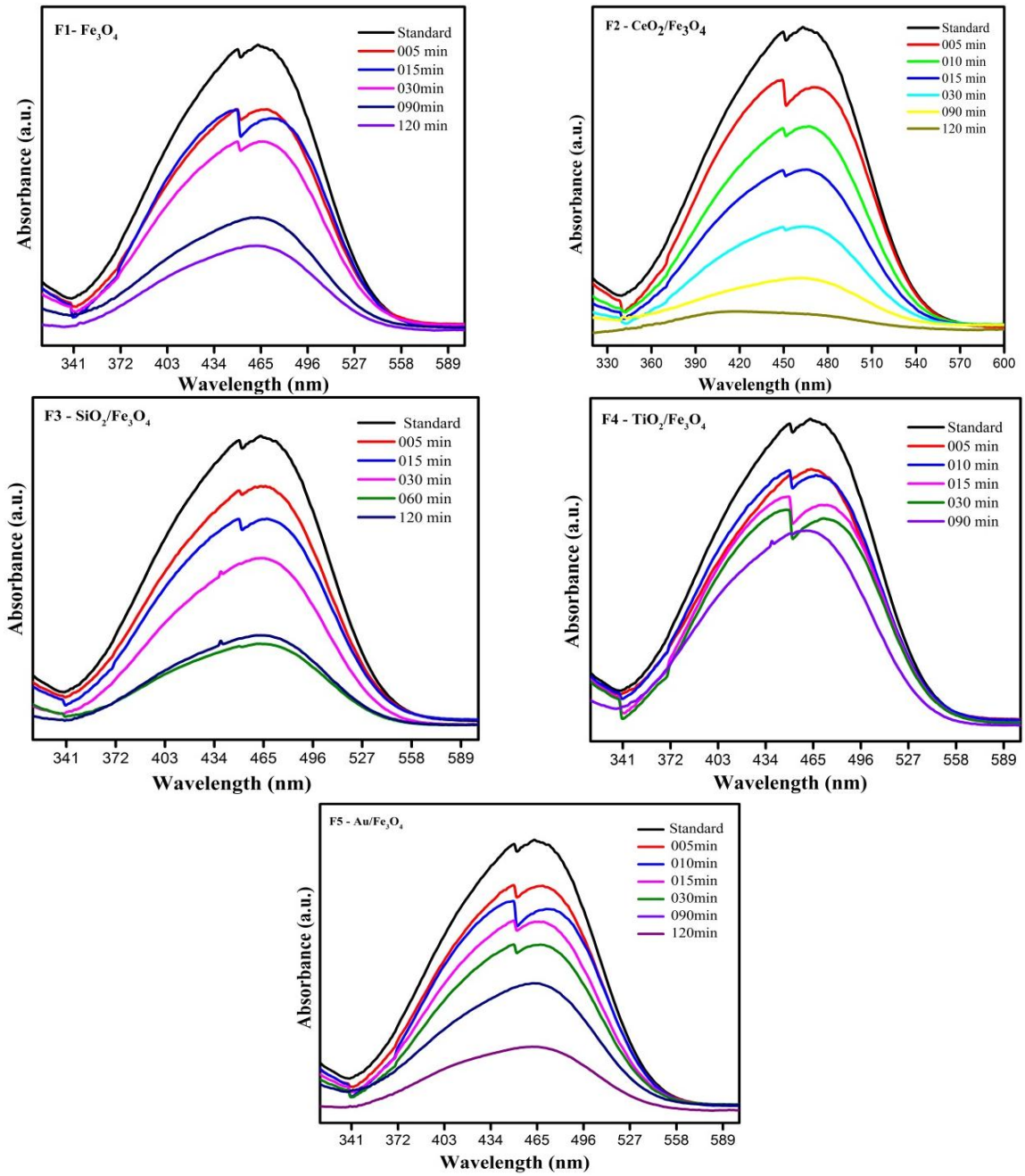

Figure 5.9. UV spectrum of methyl orange dye in visible spectrum

In this we studied the decolourization behavior of MO dye which is a cationic dye in each 30 min interval. As shown in Figure 6.1 the percentage degradation increases as degradation time increases. In case of MO the maximum degradation obtained after 20 min is 90.4% by F3 (m-CeO_2/Fe_3O_4). Whereas, percentage degradation in case of F1, F2, F4 and F5 is comparatively low as describes in Table 6.1. This can be explained by following reasons.

Firstly the bandgap of Fe_3O_4 is only 0.1eV, so the chance of electron-hole combination is very high due to which both the charge carriers do not participate in generation of radicals in the presence of solar light. This recombination is reduced by forming nanocomposites with it. But this issue is greatly reduced by ceria oxide, as consist of high content of ceria which tend to absorb solar light with high potential by forming composite with Fe_3O_4.

Secondly, the surface charge obtained for the zeta potential data over F3 is less negative (-19 mV) as compared to the others as shown in Table 5.3. So that methyl which is an anionic dye shown high absorption over F3 due to strong interaction between highly negative and nearly positive species. Stronger the interaction, better will the absorption over the surface of catalyst hence high will be degradation of organic pollutant MO dye.

Table 6.1: Showing the percentage degradation of MO and rate constant for each catalyst

Catalyst	Ratio of support and metal loading	Percentage degradation (%)	Rate Constant ($\times 10^{-1}$ min^{-1})
F1	1:0	45.5	0.1194
F2	1:1	46.2	0.1453
F3	1:1	90.4	0.1937
F4	1:1	29.7	0.0318
F5	1:1	57.7	0.1649

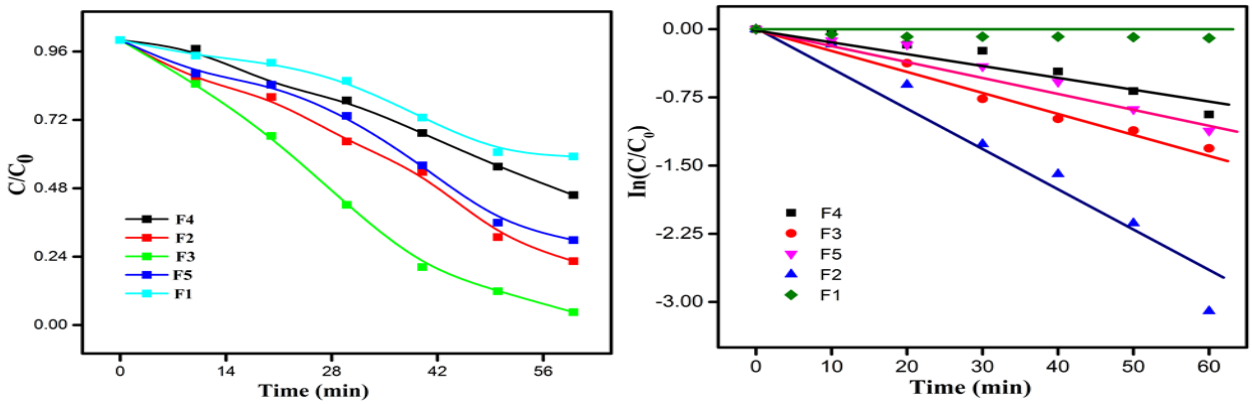

Figure 5.10: Kinetic analysis of degradation of methyl orange in presence of various metal supported Fe_3O_4 catalyst.

Methylene Blue dye

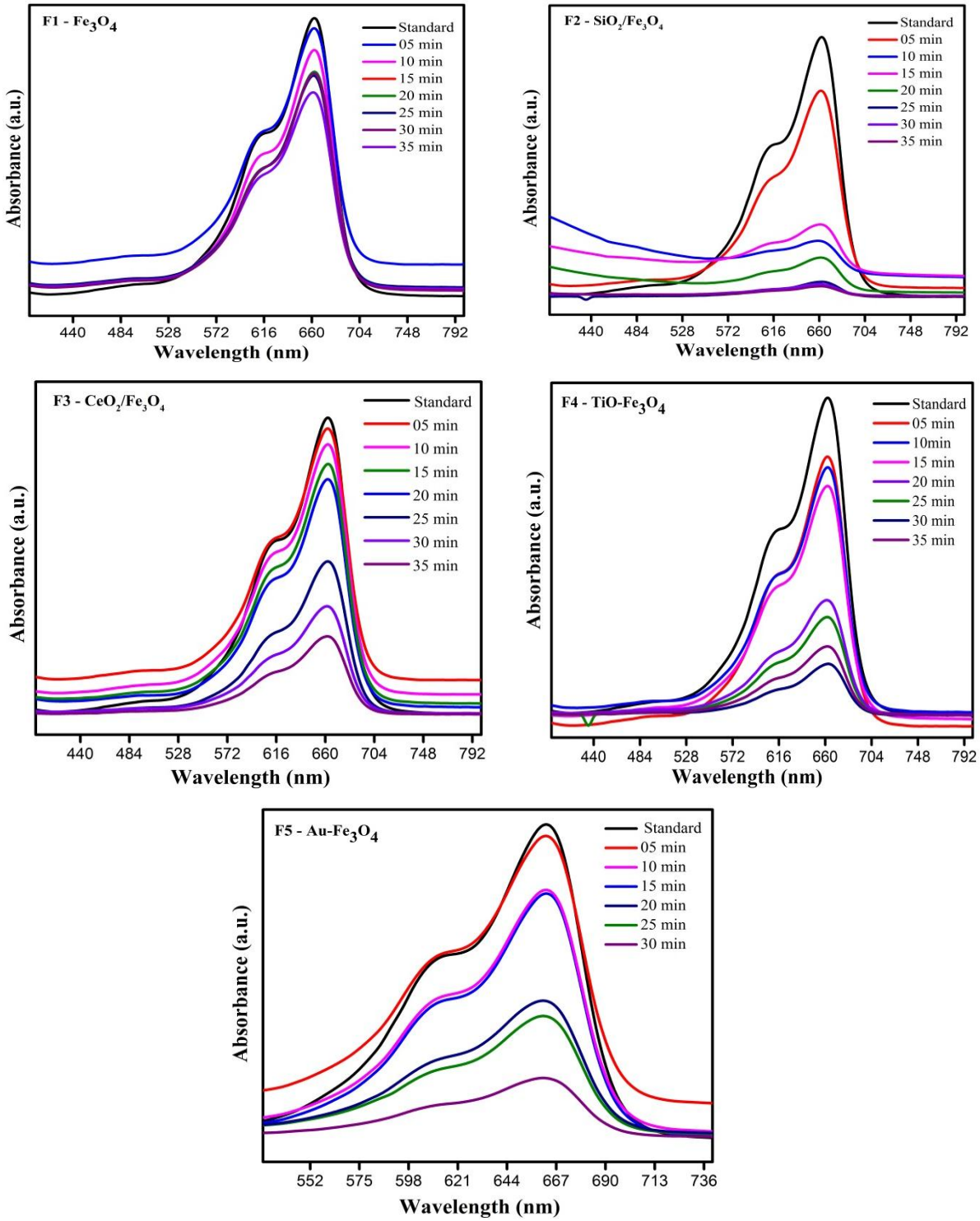

Figure 5.11: UV spectrum of methylene blue dye in visible spectrum**.**

We have also studied the decolourization behavior of cationic dye that is methylene blue. We studied its degradation rate after every 5 min interval and it is maximum degradation occur after 35 min. The maximum degradation occurred for F2 (SiO_2/Fe_3O_4) is 91.4% as shown in

Table 6.2. This is due to amorphous SiO_2 coating which having bandgap of 1.1eV which is higher than magnetite nanoparticles (0.1eV)

When a photon of light hits the surface of SiO_2, electron charge transfer takes place between bonding (Si-O) and antibonding 2p orbital of its oxygen, hence number of electrons increases in the conduction band and get transfer to the conduction band of Fe_3O_4 lying below the SiO_2, are responsible for degradation of organic pollutant.

Secondly the photocatalytic activity of a catalyst also depends upon catalyst surface. Amorphous SiO_2 provide large surface area to magnetite nanoparticles and hence increases its rate of degradation.

Table 6.2: Showing the percentage degradation and rate constant for each catalyst

Catalyst	Ratio of support and metal loading	Percentage degradation (%)	Rate Constant ($\times 10^{-1}$ min^{-1})
F1	1:0	30.1	0.0686
F2	1:1	91.4	0.1949
F3	1:1	57.7	0.1630
F4	1:1	63.6	0.1734
F5	1:1	67.2	0.1833

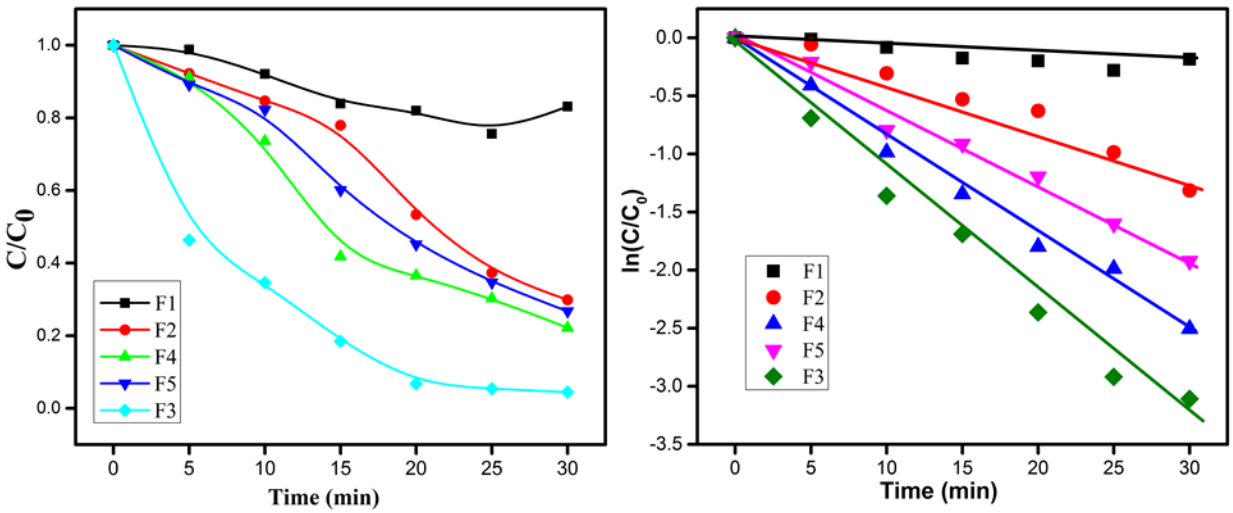

Figure 5.12: Kinetic analysis of degradation of methylene blue in presence of various metal supported Fe_3O_4 catalyst.

5.3 Kinetic Studies of Photocatalytic Degradation of both MO and MB

In order to study the kinetic behavior of these photocatalyst, the fitting of experimental data was done according to pseudo-fist order reaction as shown in figure 6.2 and figure 6.4. The graph of ln(C/Co) versus time gives a linear relationship confirmed that degradation of

methylene blue follows a pseudo first–order reaction kinetics. This can be explained according to Langmuir Hinshelwood model. The mechanism was well explained later.

$$\mathbf{ln(C_\circ/C) = kt}$$

Where, k is rate constant (min^{-1}), t is irradiation time, $C_\circ$ is initial concentration of MO and c is final concentration. From this equation the value of rate constant can be calculated for each catalyst. The calculated K value is shown in Table 6.1 and 6.2 for both methyl orange and methylene blue dye. The higher the value of rate constant k greater will be the catalytic activity of the sample. In case of MO dye the maximum rate constant is for F3 (1.937×10^{-2} min^{-1}) and it is having maximum value for F2 (1.949×10^{-2} min^{-1}) in case of MB dye.

5.4 Mechanism

Photocatalytic degradation of dye in an oxidative process in which several radical oxidative species are involved as explained in the beginning of photocatalytic studies. It is same for both anionic (methyl orange) and cationic (methylene blue).

$$\text{Catalyst} + h\nu \longrightarrow e^- + h^+$$
$$e^- + O_2 \longrightarrow O_2^-$$
$$2O_2^- + 2H^+ \longrightarrow H_2O_2 + O_2$$
$$h^+ + OH^- \longrightarrow OH$$
$$h^+ + H_2O_2 \longrightarrow OH + H^+$$
$$MB/MO + O_2^- / H_2O_2 / OH \longrightarrow \text{Intermediate} \longrightarrow \text{Degraded product}$$

Conclusions

CONCLUSIONS

The recent study shows that the surface area of magnetite nanoparticles can be increased by making M substituted magnetite nanoparticles where (M = CeO_2, SiO_2, TiO_2 and Au). The morphology of mesoporous Fe_3O_4 irregular spherical shape was determined by FESEM. The DLS data shows the particle size of m-Fe_3O_4 in nearly 100nm and surface charge over m-Fe_3O_4 is highly positive (12.5 mV) as determined by zeta potential. The mesoporous Fe_3O_4 shows high surface area (120.5 m^2g^{-1}) with SiO_2/Fe_3O_4 and carry highly negative surface charge (-19.1 mV) with CeO_2/Fe_3O_4 nanocomposites. It is also shown that due to high surface area as well as more negative charge over the surface the photocatalytic activity of magnetite nanoparticles towards the degradation of the anionic and cationic dye has been increased to greater extent. Methyl orange was degraded to (90.4%) and methylene blue was degraded to (91.4%) in just 30 min. Magnetic investigations on the samples reveal the formation of super-paramagnetic magnetite nanoparticles with high saturation magnetization with a maximum level of 36.59 emu/g. Saturation magnetization changes were explained basis of type of M loading effects on particles crystal size and ions arrangements in tetrahedral and octahedral sites.

REFERENCES

1. Sohlberg, K. (2006) Introducing the core concepts of nanoscience and nanotechnology: Two vignettes. *J. Chem. Educ, 83*(10): 1516-1530.
2. Cheng, H. N.; Doemeny, L. J.; Geraci, C. L.; Grob Schmidt, D. (2016) Nanotechnology Overview: Opportunities and Challenges. *American Chemical Society*, 1: 1-12.
3. Roco, M. C.; Bainbridge, W. S. (2005) Societal implications of nanoscience and nanotechnology: Maximizing human benefit. *Journal of Nanoparticle Research, 7*(1): 1-13.
4. Pankhurst, Q. A.; Thanh, N. T. K.; Jones, S. K.; Dobson, J. (2009) Progress in applications of magnetic nanoparticles in biomedicine. *Journal of Physics D: Applied Physics, 42*(22): 19-35.
5. Colombo, M.; Carregal-Romero, S.; Casula, M. F.; Gutiérrez, L.; Morales, M. P.; Böhm, I. B.; Parak, W. J. (2012) Biological applications of magnetic nanoparticles. *Chemical Society Reviews, 41*(11): 4306-4334.
6. Sun, S.; Zeng, H. (2002) Size-controlled synthesis of magnetite nanoparticles. *Journal of the American Chemical Society, 124*(28): 8204-8205.
7. Liang, X.; Zhong, Y.; Tan, W.; Zhu, J.; Yuan, P.; He, H.; Jiang, Z. (2013) The influence of substituting metals (Ti, V, Cr, Mn, Co and Ni) on the thermal stability of magnetite. *Journal of thermal analysis and calorimetry*, *111*(2): 1317-1324.
8. Maity, D.; Agrawal, D. C. (2007) Synthesis of iron oxide nanoparticles under oxidizing environment and their stabilization in aqueous and non-aqueous media. *Journal of Magnetism and Magnetic Materials, 308*(1): 46-55.
9. Liu, J. F.; Zhao, Z. S.; Jiang, G. B. (2008) Coating Fe3O4 magnetic nanoparticles with humic acid for high efficient removal of heavy metals in water. *Environmental science & technology, 42*(18): 6949-6954.
10. Tran, H. V.; Dai Tran, L.; Nguyen, T. N. (2010) Preparation of chitosan/magnetite composite beads and their application for removal of Pb (II) and Ni (II) from aqueous solution. *Materials Science and Engineering: C, 30*(2): 304-310.
11. Rusevova, K.; Kopinke, F. D.; Georgi, A. (2012) Nano-sized magnetic iron oxides as catalysts for heterogeneous Fenton-like reactions—Influence of Fe (II)/Fe (III) ratio on catalytic performance. *Journal of hazardous materials, 241*(2) 433-440.

12. Xu, L.; Wang, J. (2012) Magnetic nanoscaled Fe_3O_4/CeO_2 composite as an efficient Fenton-like heterogeneous catalyst for degradation of 4-chlorophenol. *Environmental science & technology*, *46*(18): 10145-10153.

13. Zhang, Y. R.; Wang, S. Q.; Shen, S. L.; Zhao, B. X. (2013) A novel water treatment magnetic nanomaterial for removal of anionic and cationic dyes under severe condition. *Chemical engineering journal*, *233*(1): 258-264.

14. Iram, M.; Guo, C.; Guan, Y.; Ishfaq, A.; Liu, H. (2010) Adsorption and magnetic removal of neutral red dye from aqueous solution using Fe_3O_4 hollow nanospheres. *Journal of hazardous materials*, *181*(1): 1039-1050.

15. Wang, Y. M.; Cao, X.; Liu, G. H.; Hong, R. Y.; Chen, Y. M.; Chen, X. F.; Wei, D. G. (2011) Synthesis of Fe 3 O 4 magnetic fluid used for magnetic resonance imaging and hyperthermia. *Journal of Magnetism and Magnetic Materials*, *323*(23): 2953-2959.

16. Khan, M. M.; Adil, S. F.; Al-Mayouf, A. (2015) Metal oxides as photocatalysts. *Chemical engineering journal*, 45(3): 462-479.

17. Lang, X.; Chen, X.; Zhao, J. (2014) Heterogeneous visible light photocatalysis for selective organic transformations. *Chemical Society Reviews*, *43*(1): 473-486.

18. Ibhadon, A. O.; Fitzpatrick, P. (2013) Heterogeneous photocatalysis: recent advances and applications. *Catalysts*, *3*(1): 189-218.

19. Wang, B.; Wei, Q.; Qu, S. (2013) Synthesis and characterization of uniform and crystalline magnetite nanoparticles via oxidation-precipitation and modified co-precipitation methods. *Int. J. Electrochem. Sci*, *8*(1): 3786-3793.

20. Hariani, P. L.; Faizal, M.; Setiabudidaya, D. (2013) Synthesis and properties of Fe_3O_4 nanoparticles by co-precipitation method to removal procion dye. *International Journal of Environmental Science and Development*, *4*(3): 336-352.

21. Petcharoen, K.; Sirivat, A. (2012) Synthesis and characterization of magnetite nanoparticles via the chemical co-precipitation method. *Materials Science and Engineering: B*, *177*(5): 421-427.

22. Xu, J.; Yang, H.; Fu, W.; Du, K.; Sui, Y.; Chen, J.; Zou, G. (2007) Preparation and magnetic properties of magnetite nanoparticles by sol–gel method. *Journal of Magnetism and magnetic Materials*, *309*(2): 307-311.

23. Daou, T. J.; Pourroy, G.; Begin-Colin, S.; Greneche, J. M.; Ulhaq-Bouillet, C.; Legaré, P.; Rogez, G. (2006) Hydrothermal synthesis of monodisperse magnetite nanoparticles. *Chemistry of Materials*, *18*(18): 4399-4404.

24. Karami, H. (2013) Heavy metal removal from water by magnetite nanorods. *Chemical Engineering Journal*, *219*(3): 209-216.

25. Nriagu, J. O.; Pacyna, J. M. (1988) Quantitative assessment of worldwide contamination of air, water and soils by trace metals. *Nature*, *333*(6169): 134-139.

26. Ranjbakhsh, E.; Bordbar, A. K.; Abbasi, M.; Khosropour, A. R.; Shams, E. (2012) Enhancement of stability and catalytic activity of immobilized lipase on silica-coated modified magnetite nanoparticles. *Chemical Engineering Journal*, *179*(4): 272-276.

27. Lei, L.; Bai, Y.; Li, Y.; Yi, L.; Yang, Y.; Xia, C. (2009) Study on immobilization of lipase onto magnetic microspheres with epoxy groups. *Journal of Magnetism and Magnetic Materials*, *321*(4): 252-258.

28. Tian, Y.; Yu, B.; Li, X.; Li, K. (2011) Facile solvothermal synthesis of monodisperse Fe_3O_4 nanocrystals with precise size control of one nanometre as potential MRI contrast agents. *Journal of Materials Chemistry*, *21*(8): 2476-2481.

29. Li, H.; Li, Y.; Zhang, Y.; Zhang, C. (2015) Facile synthesis of carbon-coated Fe_3O_4 core-shell nanoparticles as anode materials for lithium-ion batteries. *Journal of Nanoparticle Research*, *17*(9): 345-378.

30. Gao, M. R.; Zhang, S. R.; Jiang, J.; Zheng, Y. R.; Tao, D. Q.; Yu, S. H. (2011) One-pot synthesis of hierarchical magnetite nanochain assemblies with complex building units and their application for water treatment. *Journal of Materials Chemistry*, *21*(42): 16888-16892.

31. Ramesh, R.; Rajalakshmi, M.; Muthamizhchelvan, C.; Ponnusamy, S. (2012) Synthesis of Fe_3O_4 nanoflowers by one pot surfactant assisted hydrothermal method and its properties. *Materials Letters*, *70*(7): 73-75.

32. Liang, X.; He, Z.; Zhong, Y.; Tan, W.; He, H.; Yuan, P.; Zhang, J. (2013) The effect of transition metal substitution on the catalytic activity of magnetite in heterogeneous Fenton reaction: In interfacial view. *Colloids and Surfaces A: Physicochemical and Engineering Aspects*, *435*(3): 28-35.

33. Quaresma, P.; Osório, I.; Dória, G.; Carvalho, P. A.; Pereira, A.; Langer, J.; Baptista, P. V. (2014) Star-shaped magnetite gold nanoparticles for protein magnetic separation and SERS detection. *RSC Advances*, *4*(8): 3659-3667.

34. Liang, X.; Zhong, Y.; He, H.; Yuan, P.; Zhu, J.; Zhu, S.; Jiang, Z. (2012) The application of chromium substituted magnetite as heterogeneous Fenton catalyst for the degradation of aqueous cationic and anionic dyes. *Chemical Engineering Journal*, 191*(1)*: 177-184.

Kamaljeet Kaur_MSc Thesis

ORIGINALITY REPORT

%19	%	%	%19
SIMILARITY INDEX	INTERNET SOURCES	PUBLICATIONS	STUDENT PAPERS

PRIMARY SOURCES

1	Submitted to Thapar University, Patiala Student Paper	%2
2	Submitted to Higher Education Commission Pakistan Student Paper	%1
3	Submitted to Universiti Sains Malaysia Student Paper	%1
4	Submitted to Middle East Technical University Student Paper	%1
5	Submitted to Amity University Student Paper	%1
6	Submitted to Universiti Putra Malaysia Student Paper	%1
7	Submitted to Eastern Mediterranean University Student Paper	%1
8	Submitted to Universiti Teknologi MARA Student Paper	%1
9	Submitted to Curtin University of Technology	

	Student Paper	%1
10	Submitted to University of Sheffield Student Paper	%1
11	Submitted to National Institute of Technology, Rourkela Student Paper	%1
12	Submitted to University of South Australia Student Paper	%1
13	Submitted to University of Greenwich Student Paper	<%1
14	Submitted to University of Wolverhampton Student Paper	<%1
15	Submitted to ABV-Indian Institute of Information Technology and Management Gwalior Student Paper	<%1
16	Submitted to Chulalongkorn University Student Paper	<%1
17	Submitted to Tshwane University of Technology Student Paper	<%1
18	Submitted to University of Central Lancashire Student Paper	<%1

19	Submitted to PEC University of Technology Student Paper	<%1
20	Submitted to University of Strathclyde Student Paper	<%1
21	Submitted to Imperial College of Science, Technology and Medicine Student Paper	<%1
22	Submitted to University of Birmingham Student Paper	<%1
23	Submitted to University of Malaya Student Paper	<%1
24	Submitted to Jawaharlal Nehru Technological University Student Paper	<%1
25	Submitted to National University of Singapore Student Paper	<%1
26	Submitted to University of Bristol Student Paper	<%1
27	Submitted to Mahidol University Student Paper	<%1
28	Submitted to Malaviya National Institute of Technology Student Paper	<%1
29	Submitted to Fatih University	

	Student Paper	<%1
30	Submitted to King Saud University Student Paper	<%1
31	Submitted to University of Nottingham Student Paper	<%1
32	Submitted to New University of Astana Student Paper	<%1
33	Submitted to University of Witwatersrand Student Paper	<%1
34	Submitted to Universiti Kebangsaan Malaysia Student Paper	<%1
35	Submitted to Jaypee University of Information Technology Student Paper	<%1
36	Submitted to University of Bradford Student Paper	<%1
37	Submitted to Columbia University Student Paper	<%1
38	Submitted to University of Sunderland Student Paper	<%1
39	Submitted to Panjab University Student Paper	<%1
	Submitted to University of Florida	

40	Student Paper	<%1
41	Submitted to University of Wisconsin - Stout Student Paper	<%1
42	Submitted to Institute of Graduate Studies, UiTM Student Paper	<%1
43	Submitted to Universiti Tenaga Nasional Student Paper	<%1
44	Submitted to King's College Student Paper	<%1
45	Submitted to Anglia Ruskin University Student Paper	<%1
46	Submitted to Nanyang Technological University, Singapore Student Paper	<%1
47	Submitted to October University for Modern Sciences and Arts (MSA) Student Paper	<%1
48	Submitted to The University of the South Pacific Student Paper	<%1
49	Submitted to Cranfield University Student Paper	<%1

50	Submitted to Hong Kong Baptist University Student Paper	<%1

EXCLUDE QUOTES	OFF	EXCLUDE MATCHES	OFF
EXCLUDE BIBLIOGRAPHY	OFF		